Journal of Engineering Mathematics **44:** 229–243, 2002.

Analysis of radiative heat-loss effects in thermal explosion of a gas using the integral manifold method

IGOR GOLDFARB[1], VLADIMIR GOL'DHSTEIN[1], J. BARRY GREENBERG[2] and GRIGORY KUZMENKO[1]
[1]*Department of Mathematics and Computer Sciences, Ben-Gurion University of the Negev, P.O.B. 653, Beer-Sheva 84105, Israel*
[2]*Faculty of Aerospace Engineering, Technion - Israel Institute of Technology, Haifa 32000, Israel*

Received 5 September 2001; accepted in revised form 28 May 2002

Abstract. Semenov's classical model of thermal explosion in a combustible gas mixture is modified to include radiative (rather than conductive) heat-loss effects and gas-density changes. A geometrical asymptotic technique (the method of integral manifolds - MIM) is exploited to perform a qualitative analysis of the governing equations. The strength of this method lies in the compact, clear geometrical/analytical rendition and classification of all possible dynamical scenarios, in terms of the physico-chemical parameters of the system. It is found that there are two main dynamical regimes of the system: cooling regimes and fast explosive regimes. Peculiarities of these dynamical regimes are investigated and their dependence on physical system parameters is analyzed. A criterion for the occurrence of thermal explosion is disclosed. An estimate for the maximum mixture temperature is also derived analytically. It is found that, under certain operating conditions, the dynamics are such that the initial explosive stage of the process essentially behaves adiabatically before succumbing to the dominance of the radiative heat loss that brings the system down to the ambient temperature.

Key words: integral manifolds, radiative heat loss, thermal explosion.

1. Introduction

It is now a rather well established fact that radiative heat losses play a more significant role in a variety of combustion situations than was previously supposed. For example, Viskanta and Menguc [1] have extensively reviewed the effects of radiative heat transfer in combustion systems. T'ien[2] explored such effects in condensed fuel diffusion flames in the stagnation region of a forced flow, where the heat loss is from the fuel surface. This work was the first to point out that there can exist an extinction limit associated with radiation, in addition to the familiar limit stemming from too small a residence time. Sohrab *et al.* [3] discussed gas phase radiation effects in the counter-flow diffusion flame problem. Chao *et al.* [4] performed a similar analysis for the burning droplet diffusion flame problem. In both these analyses the radiation terms were replaced by equivalent Arrhenius-type expressions. Chao *et al.* [4] identified the possibility of dual turning points. In the context of premixed combustion both experimental [5, 6] and theoretical/computational [7, 8] work has highlighted the important role of radiative heat transfer. Micro-gravity experiments by Ronney [6] have enabled these effects to be more thoroughly understood, by removing masking buoyancy effects.

One, as yet unexplored, problem in the field of the mathematical theory of combustion concerns the way in which thermal radiation, emitted by a burning gas, influences the dynamics of the thermal explosion process. It is this problem that we address in this paper.

In general terms, two processes drive the behavior of the system: heat loss due to thermal radiation of the burned gas and heat release associated with an exothermic oxidation reaction. It is the competition between these processes that determines the behavior of the exploding system. We point out that, when using the term 'thermal explosion', we refer exclusively to the initial stages of the behavior of the combustible medium as its temperature begins to rise (by about 100−200K) and the aforementioned competing mechanisms are called into play. It is what takes place at this initial evolutionary period that sets the stage for the ultimate behavior of the system. Thus, we only focus on this particular episode in the combustible mixture's lifetime, rather than on its entire life history. The subsequent evolution is of no concern to us in this work, and, indeed, cannot be described by the equations we use here.

A mathematical model is developed as a system of two highly nonlinear ordinary differential equations: an energy equation and a concentration equation for the reacting gas mixture. It can be shown that the gas-phase temperature changes very quickly due to the highly exothermic reaction. On the other hand, the concentration of the combustible mixture changes relatively slowly. Therefore, the system can be considered as multiple-scale. This fact permits us to exploit a geometrical asymptotic method (MIM - integral manifold method, [9]) for qualitative analysis of the model. It thereby enables a complete classification of dynamical behavior to be given, as well as permitting critical conditions for the main dynamical regime transitions to be deduced analytically. After classifying the dynamical regimes according to different parametric regions a criterion is established for thermal explosion. In addition, an estimate for the maximum temperature attained during explosive behavior is derived. Finally, calculated results for three different fuels highlight the role of radiative heat transfer.

2. Model description

A novel modification of Semenov's classical model of thermal explosion in a combustible gas mixture is considered. The main physical assumptions of the model are as follows. We consider self-ignition of a gaseous mixture in an unconfined region. As is usual [10, Chapter 2] for the thermal explosion process we are considering here, we neglect the pressure change in the reacting mixture and its influence on the combustion process. We assume that heat transfer to the ambient is due to thermal radiation only (there are no heat losses of any other kind). The combustible component of the mixture is supposed to be deficient, whereas the concentration of the oxidizer is taken to be approximately constant. The combustion reaction is modeled as a first order, one-step highly exothermic chemical reaction.

Under these assumptions the system of governing equations reduces to an energy equation for the reacting gas (1) and a concentration equation for the reacting fuel (2):

$$c_{pg}\rho_g \frac{\mathrm{d}T_g}{\mathrm{d}t} = C_f Q_f \frac{T_{g0}}{T_g} Z \mu_f \exp\left(-\frac{E}{RT_g}\right) - q_{\mathrm{rad}}, \tag{1}$$

$$\frac{\mathrm{d}C_f}{\mathrm{d}t} = -C_f \frac{T_{g0}}{T_g} Z \ \exp\left(-\frac{E}{RT_g}\right), \tag{2}$$

where use has been made of the equation of state

$$\rho_g T_g = \rho_{g0} T_{g0} = \ \mathrm{const} \tag{3}$$

In these equations C is the concentration (kmol/m^3), ρ is the density (kg/m^3), c is the specific heat capacity (J/kg/K), q is volumetric heat loss (W/m^3 s), μ is molar mass (kg/kmol), T is

temperature (K), Q is the specific combustion energy (per unit mass) (J/kg), Z is a constant pre-exponential rate factor (s^{-1}), R is the universal gas constant and E is the activation energy (J/kmol). The notation for the subscripts is: g - gas mixture; f - combustible gas component of the mixture (fuel); p - under constant pressure; 0 - the initial state; rad - radiation.

The gas is taken to be optically thin. This situation is prevalent in many industrial applications, where the thermal radiation transfer is mainly dictated by the flammable mixture and, in turn, by its temperature. It is convenient to adopt an approximate expression for the radiative heat loss, suggested by Sohrab *et al.* [3], and successfully utilized by Chao *et al.* [4],

$$q_{\text{rad}} \approx B_r \ \exp\left(-\frac{E_r}{RT_g}\right)\chi(T - T_\infty), \tag{4}$$

rather than the well-known Stefan-Boltzman law [11, Chapter 1]. Here B_r plays the role of a constant pre-exponential factor and has dimension (J/m^3s) and E_r is a parameter similar to a conventional activation energy E (J/kmol). This form for q_{rad} was based on noting the high sensitivity of the T^4-law to temperature variations and expanding the radiation heat loss in an appropriate power series about a reference temperature (in references [3] and [4] the flame temperature). More generally, the form of Equation (4) can be derived directly from the standard expression for black-body radiation by taking some average value for the wave number of the gaseous species involved. In any event, the coefficients B_r and E_r are chosen in such a way as to minimize the difference between Equation (4) and the Stefan-Boltzman law within a given limited temperature interval. Both in references [3] and [4] and the current work the over-riding consideration for adopting Equation (4) for the radiative heat loss is mathematical tractability. The appearance of the Heaviside function, χ, in Equation (4) ensures that the radiation is cut off when the temperature of the emitting medium reaches the ambient temperature ($T_g = T_\infty$).

Initial conditions for the system of equations are:

$$T_g = T_{g0};\ C_f = C_{f0}. \tag{5}$$

The pair of Equations (1) and (2), subject to the initial conditions (5), will be used to analyze the phenomenon of thermal explosion in a combustible gas mixture with heat losses due to thermal radiation from the burned gas.

3. Classification of dynamical behaviour

To classify compactly all possible dynamical scenarios of the solutions of Equations (1) and (2) we begin by recasting the system in non-dimensional form. We define the following dimensionless variables

$$\tau = \frac{t}{t_{\text{react}}}, \quad t_{\text{react}} = Z^{-1}\exp(E/RT_{g0}), \quad \eta = \frac{C_f}{C_{f0}}, \quad \theta = \frac{E}{RT_{g0}} \cdot \frac{T_g - T_{g0}}{T_{g0}}. \tag{6}$$

Then, substituting from Equation (6) in Equations (1) and (2), we obtain

$$\gamma\frac{\mathrm{d}\theta}{\mathrm{d}\tau} = \eta\exp\left(\frac{\theta}{1+\beta\theta}\right) - \kappa_1(1+\beta\theta)\exp\left(\frac{\theta}{1+\beta\theta}\right)\exp\left(\frac{\kappa_2}{1+\beta\theta}\right)\chi(\theta - \theta_\infty), \tag{7}$$

$$\frac{\mathrm{d}\eta}{\mathrm{d}\tau} = -\eta\frac{1}{1+\beta\theta}\exp\left(\frac{\theta}{1+\beta\theta}\right), \tag{8}$$

where the following parameters appear:

$$\beta = \frac{RT_{g0}}{E}, \quad \beta_r = \frac{RT_{g0}}{E_r}, \quad \gamma = \frac{c_{pg}T_{g0}\rho_{g0}}{C_{f0}Q_f\mu_f}\beta, \quad \kappa_1 = \frac{B_r}{C_{f0}\mu_f Q_f Z}, \quad \kappa_2 = \frac{\beta_r - \beta}{\beta\beta_r}. \tag{9}$$

The initial conditions for the dimensionless Equations (7) and (8) are: $\theta = 0$; $\eta = 1$.

It is readily observed that the dynamical behavior of the system depends on five dimensionless parameters: $\beta \ll 1$, $\gamma \ll 1$, $\beta_r, \kappa_1, \kappa_2$. Parameters β and γ are the conventional parameters of Semenov's theory of thermal explosion [12] and their physical meanings are well known; β is the reduced initial temperature (with respect to the so called activation temperature E/R) and γ represents the reciprocal of the final dimensionless adiabatic temperature of the thermally insulated system after the explosion is completed. Characteristic values of these parameters (β and γ) are small compared with unity for most gaseous mixtures due to the high exothermicity of the chemical reaction and the large activation energy. Analogously, we understand β_r as some kind of initial temperature, reduced with respect to the radiative activation energy E_r. The parameters κ_1 and κ_2 are new. To elucidate the physical meaning of κ_2 we re-write it in the form

$$\kappa_2 = \frac{\beta_r - \beta}{\beta\beta_r} = \frac{1}{\beta} - \frac{1}{\beta_r} = \frac{(E - E_r)}{RT_{g0}}. \tag{10}$$

The value $\kappa_2 = 0$ distinguishes between two different cases: activation energy E less than radiation energy E_r (corresponding to $\kappa_2 < 0$), and activation energy E greater than radiation activation energy E_r (corresponding to $\kappa_2 > 0$).

The qualitative analysis of the behavior of possible solutions of Equations (7) and (8), using conventional phase-space analysis, is rendered extremely difficult due to the nature of the right-hand sides of the equations, and approximate numerical procedures must be resorted to. Alternatively, the presence of the small parameter γ on the LHS of Equation (7), such that Equations (7–8) form a singularly perturbed system, raises the possibility of using some sort of asymptotic treatment for developing solutions. In this work, we exploit a powerful technique, the so-called geometrical version of the integral manifolds method (MIM), through which the multiple-scale system under consideration is decomposed into separate studies of its component fast and slow subsystems. The advantage of this decomposition is that the subsystems have lower dimensions than the original problem. Their analysis permits a compact, clear geometrical/analytical rendition and interpretation of all possible dynamical scenarios associated with the governing equations, in terms of the physico-chemical parameters of the system. Although numerical solution of the Equations (7) and (8) is straightforward, general *analytical* parametric demarcation of the system's dynamical behaviour, such as will be presented here, is unattainable by numerical means. The reader unfamiliar with this method may refer to references [9] and [13–16] for a description of the pertinent mathematical ideas.

3.1. Shape and position of the slow curve

We have already mentioned that γ is a small parameter (due to the high exothermicity of the chemical reaction). Equation (7) describes a fast heat release process (*i.e.*, in general, the temperature θ changes rapidly relative to the concentration η), whereas Equation (8) describes the relatively slow process of concentration decay. The different rates of change of these variables suggest the geometrical version of the integral manifold method (MIM) [9, 13–15] as a suitable candidate for analyzing the equations.

We consider solutions of Equations (7) and (8) via trajectories in the $\theta - \eta$ plane. According to the integral manifold method [9] an arbitrary trajectory can be subdivided into fast and slow parts. The fast part is characterized by a constant value of the slow variable η. The slow part is quasi-stationary for the fast variable θ and is located on the integral manifold (a curve in the two-dimensional case). However, an alternative, more tractable approach is to examine the zeroth approximation ($\gamma = 0$) of the manifold. In the current problem every trajectory begins at the initial point ($\theta = 0, \eta = 1$). As long as the γ-neighborhood of the slow curve does not contain the initial point, a trajectory begins with the so-called fast motion and moves parallel to the θ-axis (in the zeroth approximation). Physically, the direction of this motion depends on the relation between heat release and heat loss terms in the RHS of Equation (7). Geometrically, its direction depends on the relative location of the slow curve to the initial point. A trajectory may reach the slow curve or pass above or below it. If a trajectory reaches a stable branch of the slow curve, its subsequent behavior essentially depends on the dynamics on this branch, which is determined by the existence of a delicate balance between heat production and radiative heat losses. Thus, the shape and location of the slow curve, and the location of the initial point relative to it define the detailed, dynamical picture.

The slow curve for Equations (7–8) is obtained by setting the RHS of Equation (7) for the fast variable (temperature) equal to zero, thus yielding

$$\Omega(\theta, \eta) = \eta - \kappa_1(1 + \beta\theta) \exp\left(\frac{\kappa_2}{1 + \beta\theta}\right) \chi(\theta - \theta_\infty) = 0. \tag{11}$$

The shape and position of the slow curve in the $\theta - \eta$ plane depend on the combination of the values of the three parameters $\kappa_1, \kappa_2, \beta$. Elementary analysis shows that the slow curve is an explicit, analytic single-valued function $\eta(\theta)$ in the $\theta - \eta$ plane, and any combination of parameters dictates its location relative to the initial point $\theta = 0$; $\eta = 1$. Now, $\kappa_2 = 0$ represents a bifurcation point for the slow curve (11). At this point of parametric space the characteristic shape of the slow curve changes sharply. For positive κ_2 the curve (11) has two branches with a vertical asymptote. For $\kappa_2 = 0$ it is simply the straight line $\eta = \kappa_1(1 + \beta\theta)$. For negative values of κ_2 it is monotonic. For further convenience we distinguish here between positive and negative values of κ_2 and analyze the slow curves in each instance.

3.1.1. $\kappa_2 > 0$

This case corresponds to the case when the activation energy of the fuel E exceeds the radiation activation energy E_r (see Equation (10)). We first determine the number and coordinates of turning points on the slow curve. The turning points **T** are points where the slow curve has a horizontal tangent, so that determination of their coordinates involves the solution of the following set of equations $\Omega(\theta, \eta) = 0$; $\partial\eta(\theta)/\partial\theta = 0$. The turning points divide the slow curve into stable and unstable parts. The stable parts attract trajectories, whereas the unstable ones repel them. Upon approaching a stable part, a trajectory begins to move along the slow curve within its γ-neighborhood (this part of the trajectory belongs to the integral manifold, which is located at a distance of $O(\gamma)$ from the slow curve). Approaching the slow curve means that two counter-directed processes (heat release due to chemical reaction and radiative heat losses) attain a fine balance. This balance is conserved during the trajectory movement along the attractive (stable) part of the slow curve. In essence, the trajectory adheres to the stable part of the slow curve. The movement along this part continues until the trajectory reaches the turning point (distinguishing stable and unstable parts) or the stationary point of the system.

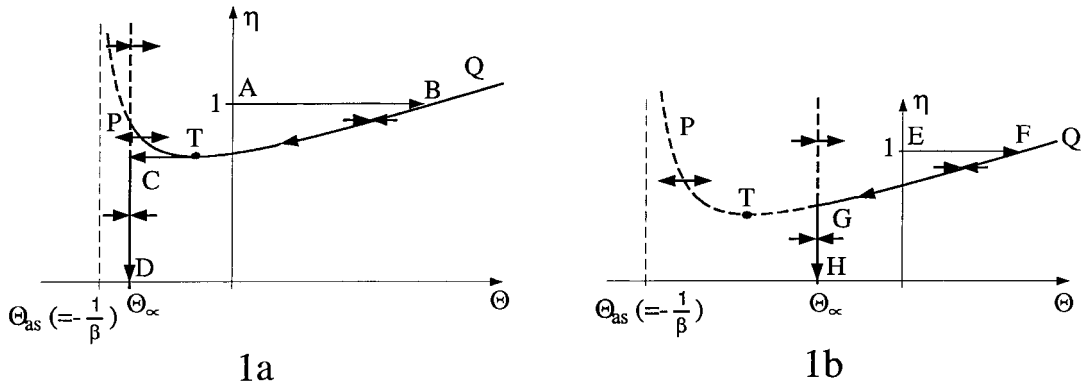

Figure 1. Two possible scenarios of thermal explosion described by Equations (7–8) when the slow curve **PTQ** has a single turning point and the initial point lies above the slow curve ($\kappa_2 > 0$, $\kappa_1 \exp(\kappa_2) < 1$). Figures 1a and 1b depict the trajectories with and without a fast cooling stage (**TC** on the Figure 1a), respectively.

Differentiating the function $\eta(\theta)$ and equating the result to zero, we reach the conclusion that the slow curve $\Omega(\theta, \eta)$ has a single turning point **T** with θ-coordinate

$$\theta_T = \frac{1}{\beta}(\kappa_2 - 1), \tag{12}$$

if $\theta_T > \theta_\infty$, or has no turning points at all if $\theta_T \leq \theta_\infty$. It is also readily seen that the slow curve $\Omega(\theta, \eta)$ has a vertical asymptote at the point $\theta = -1/\beta$, whence we conclude that the graph of the slow curve decreases when $\theta < \theta_1$ (see Figure 1, section **PT**) and increases when θ passes beyond this point ($\theta > \theta_T$, section **TQ**, Figure 1).

The presence of the ambient temperature T_∞ may be graphically illustrated by a barrier, placed at the point $\theta = \theta_\infty$, which is impenetrable by the system's trajectories. This is because the behavior of the physical system is governed by two essentially different systems of ODEs in two parts of the plane $\theta - \eta$ separated by the straight line $\theta = \theta_\infty$. To the left of this line conventional thermal explosion of an adiabatic system *without* any heat sink occurs. The Heaviside function vanishes on the RHS of Equation (7) and the temperature of the system can only increase. To the right of the line $\theta = \theta_\infty$ radiative heat losses must be accounted for. The Heaviside function in the RHS of Equation (7) equals unity here and the direction of the trajectory depends on the location of the initial point relative to the slow curve. When it lies below the slow curve, the temperature decreases and the trajectory moves towards the line $\theta = \theta_\infty$. It turns out that the part of the straight line $\theta = \theta_\infty$ lying below an intersection with the slow curve is attractive and represents an invariant manifold of a new type, which we dub a barrier manifold. This new manifold is absolutely attractive. The arrows in Figure 1 and on the following figures indicate the direction of the vector field near every part of the slow curve.

3.1.2. $\kappa_2 < 0$

The slow curve $\Omega(\theta, \eta)$ has a simpler form than in the previous case. The function $\eta(\theta)$ representing the slow curve has no turning points at all and intersects the θ-axis at the single point $\theta = -1/\beta$ (the curve **PQ**, Figure 3). It is not hard to show that, within the given parametric region, the graph of $\Omega(\theta, \eta)$ only increases ($\partial\eta(\theta)/\partial\theta > 0$)) for all meaningful (positive) values of the dimensionless concentration η and has no asymptotes.

Table 1. Classification of dynamical regimes when $\kappa_2 > 0$

$\kappa_1 \exp(\kappa_2 < 1$, Initial point above the slow curve	
(I) Figure 1a	(II) Figure 1b
(i)Fast part **AB**: temperature increases to a maximum value as exothermic chemistry dominates radiative cooling; conventional explosive regime.	(i) Fast part **EF**: temperature increases to a maximum value as exothermic chemistry dominates radiative cooling ; conventional explosive regime
(ii) Slow curve motion **BT**: till turning point **T** ($\theta_\infty < \theta_T$) is reached; balance between heat release and heat losses; delay effect.	(ii) Slow curve motion **FG**: ($\theta_T < \theta_\infty$) till $\theta = \theta_\infty$; balance between heat release and heat losses; delay effect.
(iii) Second fast part **TC**: temperature decreases sharply to θ_∞; radiative heat losses dominate.	(iii) No second fast part.
(iv) Final stage **CD**: concentration decreases to zero at $\theta = \theta_\infty$ along attractive barrier manifold.	(iv) Final stage **GH**: concentration decreases to zero at $\theta = \theta_\infty$ along attractive barrier manifold.

3.2. Classification of possible regimes

Some general remarks are in place before embarking on a detailed classification of the various dynamical regimes. The negative sign of the RHS of Equation (8) indicates that the concentration of the fuel component along an arbitrary trajectory can only decrease. A similar analysis of the RHS of Equation (7) allows us to conclude that the dimensionless temperature of the gas mixture increases ($\partial\theta/\partial\tau > 0$) and the trajectory moves in the direction of higher temperatures at some point θ_0 when the corresponding point of the trajectory lies above the slow curve ($\Omega(\theta_0, \eta_0) > 0$). Conversely, the gas temperature drops ($\partial\theta/\partial\tau < 0$) and the trajectory moves in the direction of the ambient temperature θ_∞ at point θ_0, when the point of the trajectory with coordinate θ_0 lies below the slow curve ($\Omega(\theta_0, \eta_0) < 0$.

Additionally, by substituting the coordinates of the initial point ($\theta = 0, \eta = 1$) in the expression for the slow curve (11), we can deduce whether the initial point lies above ($\Omega(0, 1) > 0$) or below ($\Omega(0, 1) < 0$) the slow curve.

We now elaborate on the possible dynamical regimes that are determined by the slow curves previously described. In the ensuing discussion the reader is advised to read the relevant tables and figures together.

3.2.1. $\kappa_2 > 0$

Recall that the slow curve in this case has a single turning point **T** (absolute minimum of the slow curve **PTQ**, Figure 1) or no turning points at all. With respect to the location of the initial point relative to the slow curve we can subdivide the parametric region under consideration into two sub-regions, corresponding to the position of the initial point being above/below the slow curve ($\kappa_1 \exp(\kappa_2) < 1$ and $\kappa_1 \exp(\kappa_2) > 1$, respectively).

Table 2. Classification of dynamical regimes when $\kappa_2 > 0$

$\kappa_1 \exp(\kappa_2) > 1$, Initial point below the slow curve		
(I) Figure 2a	(II) Figure 2b	(III) Figure 2c
(i) Fast part **AB**: turning point is above initial point; temperature decreases directly to as radiative heat losses dominate.	(i) Fast part **DE**: turning point is below initial point; temperature decreases as radiative heat losses dominate.	(i) Fast part **HJ**: turning point is below initial point; temperature decreases as radiative heat losses dominate.
(ii) No slow curve motion and delay effect.	(ii) Slow curve motion **ET**: till turning point **T** ($\theta_T < \theta_\infty$) is reached; balance between heat release and heat losses: delay effect.	(ii) Slow curve motion **JI**: ($\theta_T < \theta_\infty$) till $\theta = \theta_\infty$; balance between heat release and heat losses; delay effect.
(iii) No second fast part.	(iii) Second fast part **TF**: temperature decreases sharply to θ_∞; radiative heat losses dominate.	(iii) No second fast part;
(iv) Final stage **BC**: concentration decreases to zero at $\theta = \theta_\infty$ along attractive barrier manifold	(iv) Final stage **FG**: concentration decreases to zero at $\theta = \theta_\infty$ along attractive barrier manifold	(iv) Final stage **IK**: concentration decreases to zero at $\theta = \theta_\infty$ along attractive barrier manifold

(a) $\kappa_1 \exp(\kappa_2) < 1$. We consider a trajectory beginning at an initial point above the slow curve. Two trajectories are illustrated in Figures 1a and 1b, respectively, and their component parts with their appropriate physical meaning are succinctly summarized in Table 1. In both cases it is observed that the initial part of the trajectory corresponds to conventional explosive behavior with the exothermic chemistry dominating the heat transfer, followed by a delay effect in which the radiative heat losses balance the heat gain.

(b)$\kappa_1 \exp(\kappa_2) > 1$. Assume, now, that the initial point lies below the slow curve. The three possible trajectories under these circumstances are sketched in Figures 2a, 2b and 2c and are described in Table 2. In all cases the radiative heat loss is dominant from the initial moment, the heat release due to chemical reaction is rather small, the system cools and the gas temperature falls sharply. The subsequent scenarios may (Figures 2b, 2c) or may not (Figure 2a) involve a delay effect. The simplest of the possible slow scenarios is realized when the turning point **T** lies above the line $\eta = 1$ (Figure 2a). It is not hard to show that, if the η-coordinate of the turning point **T** is less than unity ($\eta_T < 1$), the fast part of the trajectory reaches the stable branch of the slow curve leading to the delay effect.

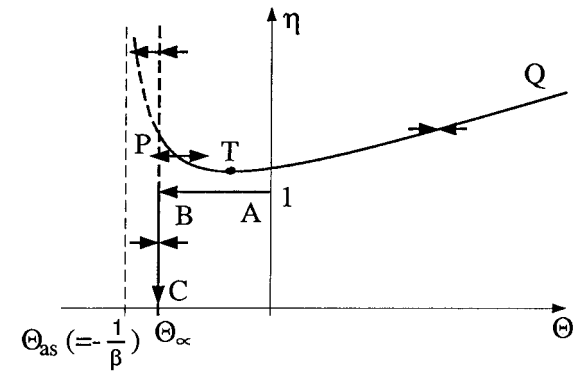

2a

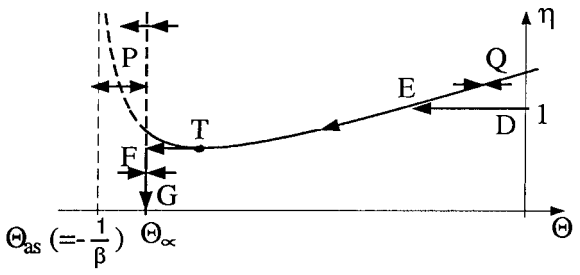

2b

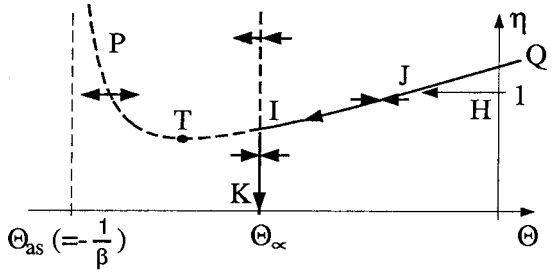

2c

Figure 2. Three possible scenarios of thermal explosion described by Equations (7–8) when the slow curve **PTQ** has a single turning point and the initial point lies below the slow curve ($\kappa_2 > 0$, $\kappa_1 \exp(\kappa_2) > 1$).

3.2.2. $\kappa_2 < 0$

In this case the slow curve $\Omega(\theta, \eta)$ has no turning points (no local maximum exists, Figures 3 and 4). Once again the location of the initial point relative to the slow curve divides the parametric region under consideration into two sub-regions according to whether $\kappa_1 \exp(\kappa_2) < 1$ or $\kappa_1 \exp(\kappa_2) > 1$.

Table 3. Classification of dynamical regimes when $\kappa_2 < 0$.

$\kappa_1 \exp(\kappa_2) < 1$	$\kappa_1 \exp(\kappa_2) > 1$	
Initial point above the slow curve	Initial point below the slow curve	
(I) Figure 3	(II) Figure 4a	(III) Figure 4b
(i) Fast part **AB**: temperature increases to a maximum value as exothermic chemistry dominates radiative cooling; conventional explosive regime.	(i) Fast part **AB**: temperature decreases directly to $\theta = \theta_\infty$; radiative heat losses dominate.	(i) Fast part **DE**: temperature decreases as radiative heat losses dominate.
(ii) Slow curve motion **BC**: till $\theta = \theta_\infty$; balance between heat release and heat losses; delay effect.	(ii) No slow curve motion and delay effect.	(ii) Slow curve motion **EF**: till $\theta = \theta_\infty$; balance between heat release and heat losses; delay effect.
(iii) Final stage **CD**: concentration decreases to zero at $\theta = \theta_\infty$ along attractive barrier manifold.	(iii) Final stage **CD**: concentration decreases to zero at $\theta = \theta_\infty$ along attractive barrier manifold.	(iii) Final stage **FG**: concentration decreases to zero at $\theta = \theta_\infty$ along attractive barrier manifold.

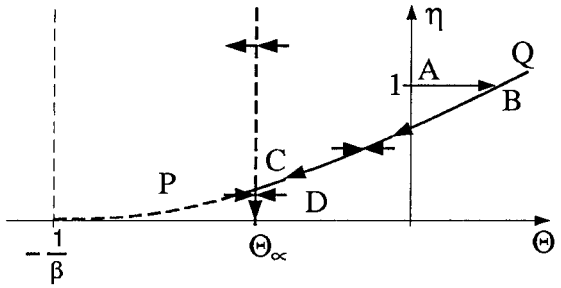

Figure 3. Possible scenario of thermal explosion described by Equations (7–8) when the slow curve **PQ** has no turning points and the initial point lies above the slow curve ($\kappa_2 < 0, \kappa_1 \exp(\kappa_2) < 1$).

(a) $\kappa_1 \exp(\kappa_2) < 1$ The single possible trajectory is shown in Figure 3 and described in Table 3. Its component parts are qualitatively similar to the scenario in Figure 1b. Initially explosive behavior occurs, followed by a delay effect and then a sharp drop in the concentration to zero.
(b) $\kappa_1 \exp(\kappa_2) > 1$. The two possible trajectories are illustrated in Figures 4a and 4b and described in Table 3. As in the parallel case of $\kappa_2 > 0$ sharp cooling of the system occurs from the outset due to radiative heat losses. Subsequently, there occurs either a delay effect (Figure 4b) to or a direct drop (Figure 4a) of the temperature to the ambient value $\theta = \theta_\infty$, at which the final stage of the process is triggered.

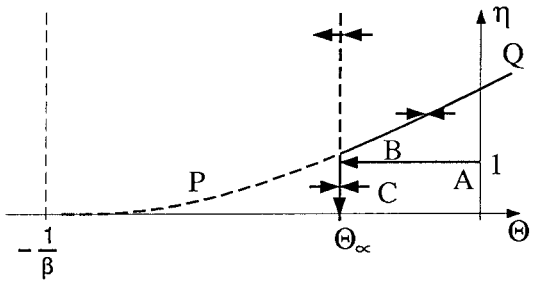

4a

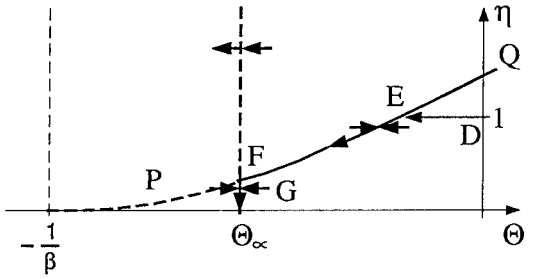

4b

Figure 4. Two possible scenarios of thermal explosion described by Equations (7–8) when the slow curve **PQ** has no turning points and the initial point lies below the slow curve ($\kappa_2 < 0, \kappa_1 \exp(\kappa_2) < 1$).

4. Characteristics of thermal exlosion

In the previous section we demonstrated that the dynamical picture of thermal explosion in a gaseous mixture in which there is thermal radiative loss is much richer than that with conventional heat losses obeying Fourier's law, for which the heat flux is linearly proportional to a temperature difference (see, for example, [17]). In particular, the conventional criterion for thermal explosion defined by a critical value of the heat-loss coefficient is transformed in the current context into a curve in the parameter plane. In addition, the maximum temperature of the gas mixture during explosion with radiant heat loss is smaller than that obtained in the case with conductive heat losses.

4.1. THERMAL EXPLOSION CRITERION

The aforedescribed analysis allows the establishment of conditions that distinguish explosive regimes from slow ones, and thereby to determine a criterion for explosion. We have already found that explosive behavior of the mixture temperature occurs when $\kappa_1 \exp(\kappa_2) < 1$. The appearance of two dimensionless parameters in this inequality is linked to the two independent parameters, the pre-exponential factor B_r and the radiative activation energy E_r that appear in the definition of the radiative heat loss term, see Equation (4). These two parameters dictate the intensity of the radiative heat flux from the burned gas to the ambient. Figure 5 depicts a curve representing the criterion for thermal explosion in the $\kappa_1 - \kappa_2$ parameter plane.

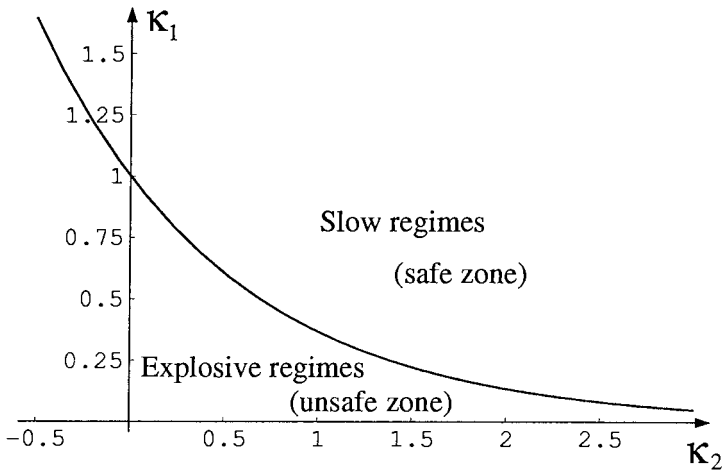

Figure 5. Regime map (safe - unsafe) in the $\kappa_2 - \kappa_1$ parameter plane.

4.2. MAXIMUM EXPLOSIVE TEMPERATURE

It is of great interest to derive an approximate expression for the maximum temperature of the burning system that can be attained in the process of thermal explosion. To get a rough estimate of the magnitude of this parameter, we explore the quasi-stationary approximation for the slow variable η. Substituting the initial value of the dimensionless concentration η in Equation (11) for the slow curve we obtain the following equation from which the maximum temperature can be assessed

$$1 - \kappa_1(1 + \beta\theta_{\max}^{(0)}) \exp\left(\frac{\kappa_2}{1 + \beta\theta_{\max}^{(0)}}\right) = 0 \tag{13}$$

This transcendental equation cannot be solved analytically. However, if the conventional Frank-Kamenetskii approximation [10, Chapter 2], $\beta\theta_{\max}^{(0)} \ll 1$, is applicable, an approximate expression for the maximum temperature $\theta_{\max}^{(0)}$ is derived in the form

$$\theta_{\max}^{(0)} \approx \frac{1 - \kappa_1 \exp(\kappa_2)}{\beta\kappa_1(1 - \kappa_2)\exp(\kappa_2)} \tag{14}$$

4.3. RESULTS

It is of interest to estimate the effect of thermal radiation losses for some specific cases. We make use of the data of Chao *et al.* [4]. They assumed that Planck's mean absorption coefficient κ is the molar average value of the mixture in the radiation region. In our case, due to the assumption that the fuel is the deficient reactant, the gaseous mixture can be considered as consisting of CO_2, H_2O and N_2. Furthermore, since N_2 is very non-radiative in comparison to CO_2 and H_2O, we can restrict ourselves by taking into account the two latter components only. Therefore, the Planck's mean absorption coefficient κ reads

$$\kappa = x_{CO_2}\kappa_{CO_2} + x_{H_2O}\kappa_{H_2O}, \tag{15}$$

where x_i is the molar fraction of the i-th mixture component. For the stoichiometric burning of heptane in air, Chao *et al.* calculated a value of $\kappa = 0{\cdot}8\ \mathrm{m}^{-1}$ on the basis of CO_2 and H_2O

Table 4. Thermophysical data for n-decane, n-heptane and tetralin

Property	n-decane	n-heptane	tetralin
Heat capacity c, J/kg/K	1050	1050	1256
Latent heat L, J/kg	$3{\cdot}21 \times 10^5$	$3{\cdot}2 \times 10^5$	$3{\cdot}17 \times 10^5$
Initial temperature, K	1100	1100	1100
Molar mass μ_f, kg/kmol	142	100	132
Combustion energy Q, J/kg	$4{\cdot}42 \times 10^7$	$4{\cdot}54 \times 10^7$	$1{\cdot}266 \times 10^7$
Activation energy E, J/kmol	$1{\cdot}257 \times 10^8$	$1{\cdot}257 \times 10^8$	2×10^8
Thermal conductivity λ, W/m/K	0·0193	0·0193	0·084
Preexponential factor A, 1/s	$0{\cdot}95 \times 10^7$	$0{\cdot}95 \times 10^7$	$1{\cdot}15 \times 10^8$

absorption coefficients evaluated at 1 atm and 2,000 K. By performing a best fit of the fourth-power law by an exponential function they extracted a value of 8,000 K for the so-called equivalent radiation temperature E_r/R (this approximation is valid within a restricted range of gas temperatures 1,600 K $\leq T_g \leq$ 2500 K) which corresponds to a radiation activation energy $E_r = 66{\cdot}5$ MJ/kmol. For the radiation pre-exponentional factor they obtained the value $B_r = 16$ kW/m^3.

Using these values of the radiation parameters, we find that the absolute value of κ_1 is rather small, of the order of 10^{-10}. For the second dimensionless parameter κ_2, characterizing the relation between radiative and conventional activation energies, we obtain a value of 17·5. In terms of the detailed classification of regimes we have analysed these values correspond to case (I) shown in Figure 1a. The small value of parameter κ_1 implies a location about the right branch of the slow curve **TQ**, very close to the temperature axis, so that, correspondingly, the intersection point between the trajectory and the slow curve lies very close to the θ-axis. Therefore, under this particular set of conditions, at the point **B** (Figure 1a) the gaseous fuel is almost completely consumed before the radiative losses play a noticeable role in the system's dynamics. Under these circumstances a measure of the deviation of the maximum temperature brought on by the radiative heat losses can be assessed using $(\theta_{\text{ad.}} - \theta_{\max}^{(0)})/\theta_{\text{ad.}}$, where $\theta_{\text{ad}} = \gamma^{-1}$ is the adiabatic temperature of the system in the absence of any thermal losses. It is readily seen that this expression is a function of the dimensionless parameter κ_1 and extremely sensitive to the value of κ_2.

Analysis of the definitions of the parameters κ_1, κ_2 shows that the influence of the thermal radiation changes strongly with the physico-chemical properties of the fuel and depends on the radiative properties of the original gaseous mixture. Detailed numerical simulations confirmed this conclusion. For example, for the stoichiometric combustion of n-decane in air the relative influence of the radiation phenomenon is 0·015%, whereas for combustion in an atmosphere of CO_2 (*i.e.* more radiative CO_2 is substituted for non-radiative hydrogen in the air) this value is equal to 0·09%. The initial temperature of the mixture was taken to be 1100 K; other parameters used for the calculations are presented in Table 4. A qualitatively different picture is obtained for the thermal explosion of tetralin (a fuel with a larger activation energy and smaller combustion energy than that of normal hydrocarbons), for combustion of which the radiative losses *cannot* be ignored from the very beginning of the process. For the stoichio-

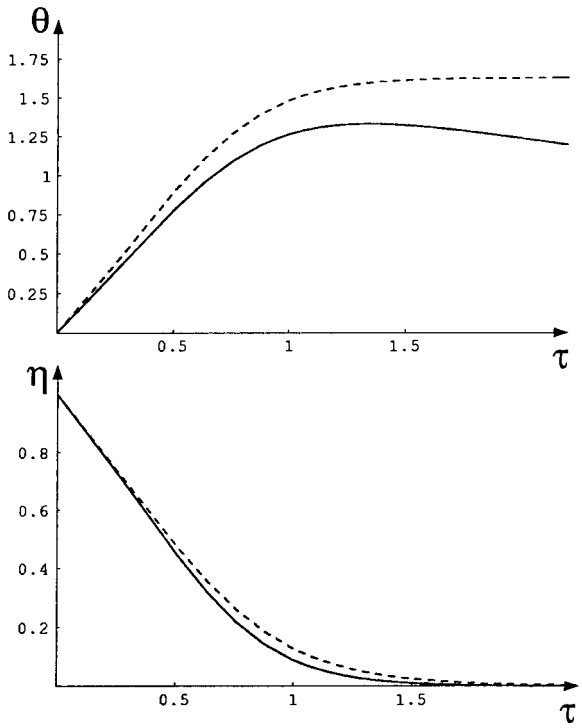

Figure 6. Time histories of the dimensionless temperature (upper) and concentration (lower). Solid line represents result of calculation of the full system (7−8), dotted line depicts results of calculation of the adiabatic version of the system (7−8) (without radiative losses on RHS of Equation (7)).

metric combustion of tetralin in air the relative influence of the radiation phenomenon is 4·3%, whereas for combustion in an atmosphere of CO_2 this value tends to a third (28%). In Figure 6 the evolution with time of the temperature and the concentration of tetralin are illustrated, with and without radiative heat losses (the continuous and broken lines, respectively). From early in the system's development radiation plays a major role in the departure of the temperature from the adiabatic profile. In contrast, for n-decane and n-heptane (curves not shown here) this divergence was barely distinguishable.

5. Conclusions

A novel modification of Semenov's classical problem of thermal explosion of a gaseous mixture in the presence of radiative heat transfer from the burning gas to the ambient is considered and analysed. The model takes into account heat release due to the exothermic oxidation of gaseous fuel, gaseous fuel consumption as a result of a chemical reaction, and radiative heat losses. The mathematical formulation involves a singularly perturbed system of two nonlinear ordinary differential equations. A geometrical version of the integral manifold method is used for the qualitative analysis of the dynamics of this system. The dynamic behavior of the system is completely classified according to the values of five key dimensionless parameters: $\beta, \gamma, \kappa_1, \kappa_2, \beta_r$ under the additional assumption that the first two are small with respect to unity. Two main types of dynamic behavior are found for the system: conventional fast explosive regimes (slow cooling after fast temperature growth) and fast cooling (cooling is

split into a relatively fast first stage followed by a period of relatively slow cooling). Possible variations of these two types of system dynamics are analysed. An analytical estimate for the maximum explosive temperature is derived and the relative importance of the radiative heat losses is discussed. The dependence on the physical parameters of the system of the delay time until radiative effects become appreciable is investigated. The analytical study and numerical examples for three fuels, n-decane, n-heptane and tetralin, indicate the critical role of the fuel type and the ambient conditions in determining the influence of thermal radiation on the maximum explosive temperature. It is shown that in the case of normal hydrocarbons the effects of thermal radiation can be largely ignored at the fast (explosive) stage of the thermal explosion, whereas for tetralin these effects are significant even at this stage.

Acknowledgement

J.B.G. wishes to acknowledge the partial support of the Lady Davis Chair in Aerospace Engineering and the Technion Fund for the Promotion of Research. Thanks are also due to Dr. M. Lev for some very instructive conversations.

References

1. R. Viskanta and M.P. Menguc, Radiation heat transfer in combustion systems. *Progr. Energy Combust. Sci.* 13(2) (1987) 97–160.
2. J.S. T'ien, Diffusion flame extinction at small stretch rates: the mechanism of radiative loss. *Combust. Flame* 65 (1986) 31–34.
3. S.H. Sohrab, A. Liñan and F.A. Williams, Asymptotic theory of diffusion-flame extinction with radiant loss from the flame zone. *Combust. Sci. Technol.* 27 (1982) 143–154.
4. B.H. Chao, C.K. Law and J.S. Tien, Structure and extinction of diffusion flames with flame radiation. *Proc. Combust. Inst.* 23 (1991) 523–531.
5. L. Honda, and P.D. Ronney, Effects of ambient atmosphere on flame speed at microgravity. *Combust. Sci. Technol.* 133 (1998) 267–291.
6. P.D. Ronney, Understanding combustion processes through microgravity research. *Proc. Combust. Inst.* 27 (1998) 2485–2506.
7. J.D. Buckmaster, M. Smooke and V. Giovangigli, Analysis and numerical modeling of flame-balls in hydrogen-air mixtures. Combust. *Flame* 94 (1993) 113–124.
8. M.S. Wu, J.B. Liu and P.D. Ronney, Numerical simulation of diluent effects in flame ball structure and dynamics. *Proc. Combust. Inst.* 27 (1998) 2534–2550.
9. V.M. Gol'dshtein and V.A. Sobolev, (1992) Singularity theory and some problems of functional analysis. *AMS Translations*, Series 2 153 (1992) 73–92.
10. D.A. Frank-Kamenetskii, *Diffusion and Heat Exchange in Chemical Kinetics*. New York: Plenum Press (1969) 574pp.
11. M. F. Modest, *Radiative Heat Transfer*. New York: McGraw-Hill (1993) 832pp.
12. N.N. Semenov, Zur Theorie des Verbrennungsprozesses. *Z. Phys* 48 (1928) 571–581.
13. V.I. Babushok. and V.M. Gol'dshtein, Structure of thermal explosion limit. *Combust. Flame* 72 (1988) 221–226.
14. B.B. Strygin and V.A. Sobolev, *Decomposition of Motions by the Integral Manifolds Method*. (in Russian) Moscow: Nauka (1988) 256pp.
15. I. Goldfarb, V. Gol'dshtein, G. Kuzmenko and J.B. Greenberg, On thermal explosion of a cool spray in a hot gas. *Proc. Combust. Inst.* 27 (1998) 2367–2371.
16. N. Fenichel, Geometric singular perturbation theory for ordinary differential equations. *J Diff. Equ.* 31 (1979) 53–98.
17. V. Gol'dshtein, A. Zinoviev, V. Sobolev and E. Shchepakina, Criterion for thermal explosion with reactant consumption in a dusty gas. *Proc. Royal Soc. London*, Series A 452 (1996) 2103–2119.